Fast-switching cycle times for BIMA's A array

R.L. Akeson

ABSTRACT

Fast switching cycle times to minimize atmospheric phase fluctuations are calculated for conditions applicable to BIMA A array observing. The optimal cycle time is defined as having the lowest total noise from thermal and atmospheric contributions. It is assumed that decorrelation from the atmosphere can be partially corrected using observations of a test calibrator. Guidelines are given for cycle times for various array, source and atmospheric parameters.

1. Introduction

High resolution interferometry at millimeter wavelengths is limited by phase fluctuations caused by atmospheric water vapor turbulence. These fluctuations can introduce an 'effective seeing' larger than the resolution provided by the actual baseline lengths as the phase fluctuations will cause varying amounts of decorrelation (for more details see Wright 1996, Lay 1997). In millimeter interferometry, the technique of phase referencing, in which a known source is occasionally observed, is generally used to remove instrumental and atmospheric phase. For a cycle time t_{cyc}, defined as the time between observations of the phase reference, this technique can only measure phase variations with periods longer than $2 * t_{cyc}$, the Nyquist limit. Any phase fluctuations with periods less than $2 * t_{cyc}$ will remain in the data as residual phase errors, resulting in decorrelation. On baselines up to ~100 meters, phase referencing every 20–30 minutes is sufficient in most weather conditions to remove most of the atmospheric phase. However, at much longer baselines, the phase fluctuations increase and traditional phase referencing is not adequate. One method to minimize the effect of the atmospheric fluctuations is to decrease t_{cyc} to a few minutes or less. This technique is sometimes referred to as fast switching. The goal of this memo is to produce recommendations for fast-switching cycle times for A array observations at BIMA.

The optimal cycle time will depend on several factors, including the temporal and spatial distributions of fluctuations in the atmosphere, the slew rate and sensitivity of the telescopes, and the location and strength of available calibration sources. The optimal cycle time will also depend on what measurements are desired from the target observations: t_{cyc} for measuring the flux of a known point source will be different than t_{cyc} for resolving a target with low surface brightness. As strong target sources can utilize self-calibration to improve the gain calibration, I concentrate on weaker targets (flux < 200 mJy).

The model for the atmospheric and array parameters is described in §2. The criteria for determining the optimal cycle time are derived in §3. The results of the calculations are given in §4 for varying values of the target, array and atmospheric parameters. General recommendations for fast switching cycle times are summarized in §5.

2. Atmospheric and array model

A full simulation of atmospheric effects on interferometric observations is a complicated problem. One possible method would be: 1) generate model visibilities for the target and calibrator, 2) add synthetic phase noise to both the target and calibrator visibilities with the correct magnitude and correlation to simulate the atmosphere passing over the array, and 3) calibrate the target data and generate an image. The second step in this prescription is the most difficult, as several crucial atmospheric variables, including the altitude and thickness of the turbulent layer and the wind speed as a function of height are not well known.

To simplify the problem of simulating atmospheric effects on high resolution observations, I use a model of the temporal power spectrum of the fluctuations developed by Lay (1997, see paper for details). The phase fluctuations introduced by the atmosphere depend on the baseline length and the time scale. The power spectrum is scaled for a given baseline length and atmospheric conditions. The normalization is provided by the rms path in 10 minutes on a 100 meter baseline, which is the output measurement of the phase monitor (Lay 1998). The residual rms phase at 100 GHz after phase calibration and the resulting decorrelation for this model are shown in Figure 1 as a function t_{cyc}.

The properties for this model atmosphere are:

- Altitude of turbulent layer = 1 km
- Thickness of turbulent layer = 500 m
- Wind speed = 5 m/s
- Elevation = 45 degrees

As demonstrated in Figure 1, the decorrelation can be significant even on time scales of less than 1 minute. The decorrelation within the integration time on a given object can be decreased by recording the data every 5 to 10 seconds. In the following calculations, I have assumed that the data is recorded every 5 seconds and have neglected the decorrelation within that time. On a 1 km baseline, the decorrelation in 5 seconds is only 3% for a rms path of 400 μm on the phase monitor. To properly correct for this decorrelation, all sources (target, gain calibrator and test calibrator) should have the same data record length. I have also assumed that the gain does not vary during the track.

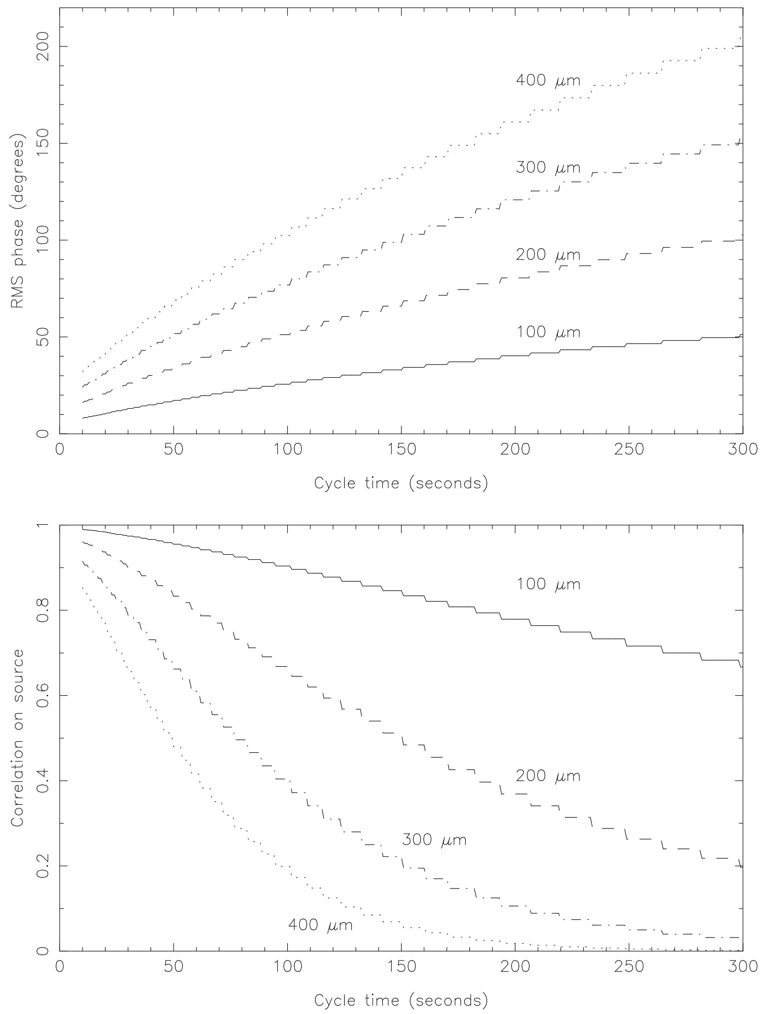

Fig. 1.— The residual rms phase at 100 GHz after phase referencing and the resulting correlation on the target as a function of cycle time and at 4 values for the rms path as measured by the phase monitor. The steps in the curves are due to the finite time resolution of the model atmosphere.

The array parameters used are:

- Baseline length = 1 km
- Slew rate = 1.5 degrees/sec
- Settle time = 4 seconds
- Minimum int time = 5 seconds
- Track length = 8 hrs
- Bandwidth = 800 MHz
- λ = 3mm

Only continuum observations at λ=3mm are considered in these calculations. The 1 km baseline was chosen as representative for A array. For the atmospheric model used here, the rms phase after phase referencing has been applied is constant with baseline length for baselines greater than ∼250 meters (Figure 2). For baselines shorter than this, the atmospheric contribution to the noise will be overestimated. The value for the settle time was determined from observations by J. Welch.

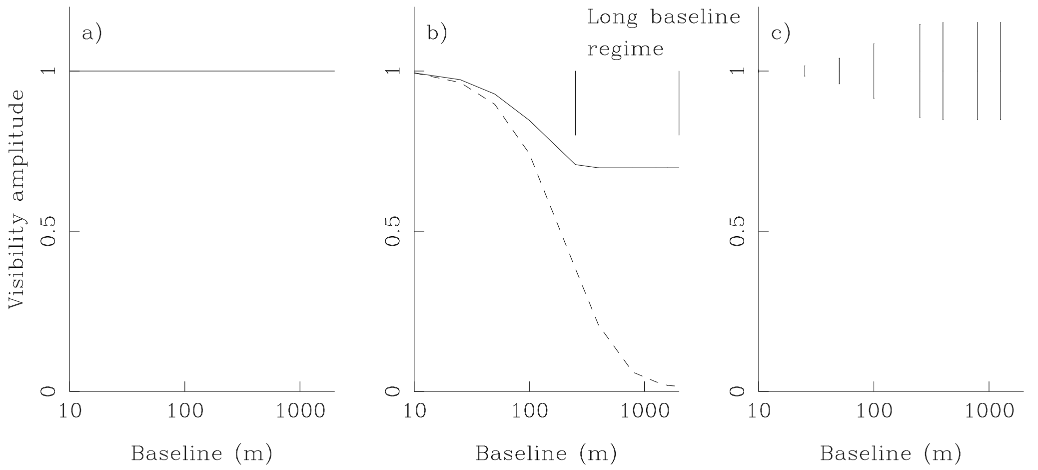

Fig. 2.— a) The visibility amplitude versus baseline for a unresolved source. b) The visibility amplitude for the same source including atmospheric decorrelation corresponding to an rms path of 200 μm and t_{cyc} of 2 minutes before (dashed line) and after phase referencing (solid line) is applied. Note that the decorrelation is constant for baselines longer than ∼250 meters after phase referencing is applied. c) The uncertainties resulting from the estimation of the decorrelation (see §3.1).

3. Criteria for optimization

The optimal cycle time is a trade-off between time on the target, which decreases the thermal noise, switching quickly between the calibrator and the target, which decreases the atmospheric phase noise, and the phase error per cycle due to thermal noise in the calibrator measurement. The residual atmospheric phase after calibration depends on the difference between the fluctuations in the direction to the target and in the direction to the calibrator. During the cycle time, the wind blows the turbulent layer over the array a distance of the wind speed times t_{cyc}. The second distance component is the physical distance within the turbulent layer between the line-of-sight to the target and the line-of-sight to the calibrator. As the wind and target-calibrator distance are really vector quantities with respect to the turbulence, the scalar addition used here is a conservative estimate. This approximation is only valid on baselines longer than the target-calibrator distance in the turbulent layer. The wind speed * t_{cyc} term dominates for most cases considered in §4.

3.1. Decorrelation

The total phase error (atmospheric + calibrator) results in decorrelation of the target visibilities. As seen in Figure 1, this decorrelation increases quickly with longer time scales and in worse atmospheric phase conditions. A array observations which hope to resolve small scale structure should therefore include a test calibrator source, as near to the target source as possible. There are 2 approaches in observing the test calibrator: 1) include it within every cycle, or 2) after several cycles on the target, observe the test calibrator using the same integration time as for the target. If the amount of decorrelation changes rapidly in time, then the first method may be better; however, only the second method will measure the decorrelation over the total cycle on the target. I use the second method in the following calculations. I also assume that the test calibrator and the target are located the same distance from the phase calibrator.

In using a test calibrator to measure the decorrelation, there will be an error from the thermal noise on the test calibrator and from temporal and spatial variations in the decorrelation (i.e. the decorrelation in a given 30 seconds may be different than the decorrelation in the next 30 seconds). To study how the value of the decorrelation varies over time, I analyzed the phase monitor data taken in April and May 1998, comprising 10 minute rms path measurements. I averaged every 6 measurements (1 hour) and found the rms within an hour. This result is the rms of the rms path; I will refer to this value as rms_{rms} and to the original data as the rms path measurements. Figure 3 shows the rms_{rms} over 1 hour versus the average rms path, for rms path values below 800 μm. The value of the rms_{rms} scales roughly linearly with the average rms path. The line corresponds to an rms_{rms} equal to 25% of the average rms path, and is an estimate of the relationship rather than a formal fit. While this line is slightly high for the best weather (100μm), it fits well at 200–400 μm rms path. Rms path values greater than 400 μm are not considered here because the decorrelation is too large on long baselines. This correspondence between the rms path and the rms_{rms} applies to variations in atmospheric conditions on time scales from 10 minutes to 1 hour. For fast switching observations, the fluctuations on scales as short as 10 seconds are important. As there are no direct measurements on shorter time scales, I have assumed that the relationship between the rms_{rms} and the average rms path seen on 10 minute to 1 hour time scales also applies to shorter time scales.

The total decorrelation is

$$d = 1 - e^{-\phi^2/2}, \tag{1}$$

where ϕ is the total rms phase per cycle, composed of the atmospheric rms ϕ_{atm} and the error in the calibrator measurement due to thermal noise, σ_{cal}/F_{cal}, added in quadrature

$$\phi^2 = \phi_{atm}^2 + (\sigma_{cal}/F_{cal})^2. \tag{2}$$

From Figure 3, I estimate that ϕ_{atm} can be measured to within 25% using the test calibrator observations. The remaining rms phase will result in uncertainties in the target data, as the decorrelation can be either higher or lower than as measured on the test calibrator (Figure 2c).

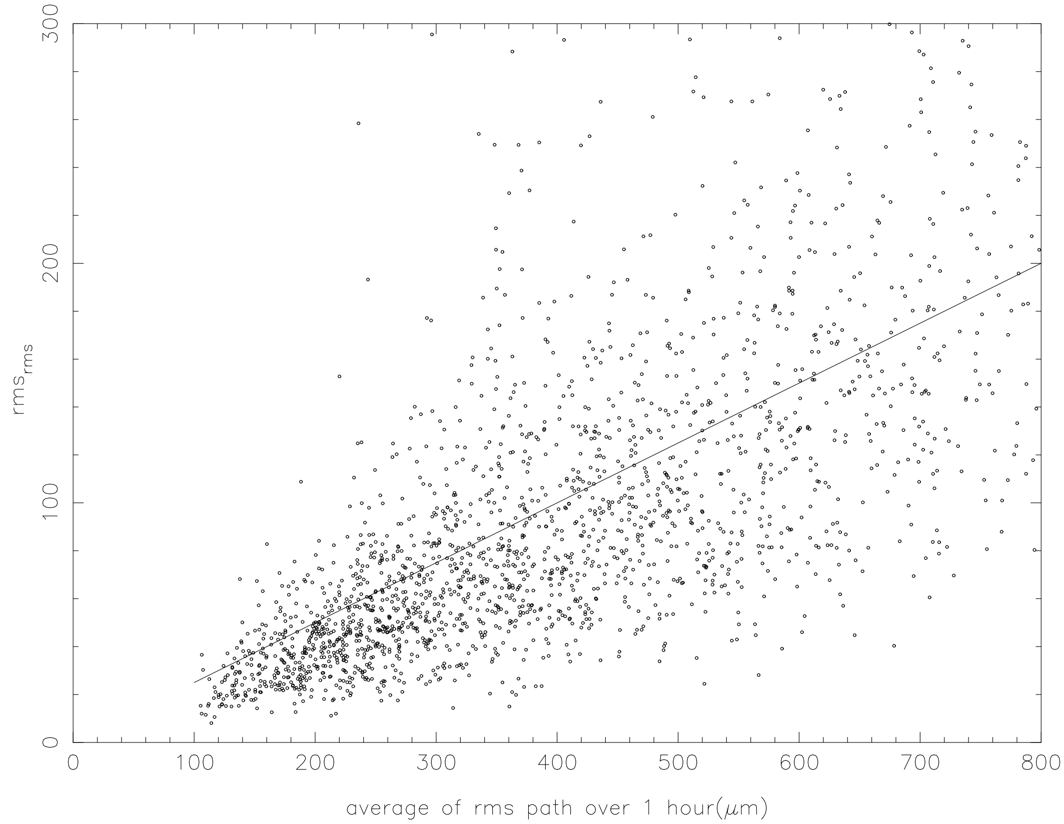

Fig. 3.— The rms_{rms} plotted against the average rms path (10 minute measurements from the phase monitor) over 1 hour scales. The line corresponds to the rms_{rms} equal to 25% of the average rms path.

This uncertainty will be expressed as a fraction of the decorrelation, f_d,

$$f_d = \Delta\phi * \phi * e^{-\phi^2/2}. \tag{3}$$

As the decorrelation is an exponential, f_d, varies with the value of the decorrelation. For example, if ϕ is 25°, then the 25% estimation error results in $f_d = 0.044$ while at $\phi = 50°$, $f_d = 0.13$. The total uncertainty used to optimize the cycle time is

$$\sigma_{total} = \Big((\frac{\sigma_{target}}{e^{-\phi^2/2}})^2 + (\frac{\sigma_{test} * F_{target}}{F_{test} e^{-\phi^2/2}})^2 + (f_d * F_{target})^2 \Big)^{1/2} \tag{4}$$

where σ_{target} is thermal noise for the target and σ_{test} is the thermal noise on the test calibrator. The second term is the error due to thermal noise in measuring the decorrelation of the test calibrator and the third term is the uncertainty introduced in estimating the decorrelation.

In real observations, baselines of different orientations and lengths are sensitive to different size structures in the target emission. For example, shorter baselines are sensitive to more of the total flux for an extended source and the error in measuring the total flux is not determined by the combined noise for all visibilities. For the optimization calculations, determination of the appropriate thermal noise is important. One way of viewing this problem is to consider the flux distribution in the uv plane. For a point source, the flux is constant and only one uv bin is needed to measure the amplitude. Thus, all the visibilities are combined in determining the noise of this bin. If the target is resolved (assuming a symmetric source at the point center) then the amplitude will decrease at larger uv distances. If the total number of visibilities is divided into n bins with equal numbers of visibilities, the thermal noise in each bin is $\sqrt{n}$ times the noise for all the visibilities combined. In calculating the thermal noise I assume 45 identical baselines, but the visibilities are divided into a specified number of 'bins' and σ_{target} and σ_{test} are scaled appropriately. This simplification neglects any correlations between phase errors that may occur for visibilities in adjacent uv cells. A much more detailed simulation, such as the one described at the beginning of §2 would be necessary to study this effect.

4. Results

4.1. Test case

As the optimal cycle time will depend not only on the atmospheric conditions, but also on the target characteristics, I have chosen a test case which falls in the middle of the range of possible source models. The visibilities are divided into 3 bins. A real astronomical example of this case would be looking for evidence that a source is resolved by comparing the flux on different baselines. For the optimization, I have chosen a target flux of 100 mJy, test calibrator flux of 400 mJy and a 1 Jy phase calibrator located 10 degrees from the target. For these parameters, the optimal cycle time was calculated as a function of system temperature and rms path as measured by the phase monitor (Figure 4). As expected, the optimal cycle time decreases for higher values of the rms path. At higher system temperatures, relatively more time must be spent on the target (panel d) to make up for the increased thermal noise, although the resulting uncertainties are higher than at low system temperatures (panel f). The optimal cycle time for good A array conditions (200 μm rms path and 300 K T_{sys}) is 45 seconds with 9 seconds on the calibrator and 15 seconds on the target. During the 1997-98 observing season at Hat Creek, the rms path was 200 μm or lower during 40% of the time used for observing in the best two months, November and December (Akeson, 1998). For low system temperatures and high rms path, the cycle times are limited by the imposed 5 second minimum integration time.

4.2. Changing assumed values

To study the effect of the assumed values for the target, calibrator, and atmospheric variables, I changed each value one at a time for the case of T_{sys}=300 K and rms path of 200 μm. The optimal cycle time, as well as the uncorrected target correlation and total uncertainty are given in Table 1 for variations in the target and calibrator parameters and in Table 2 for the atmospheric

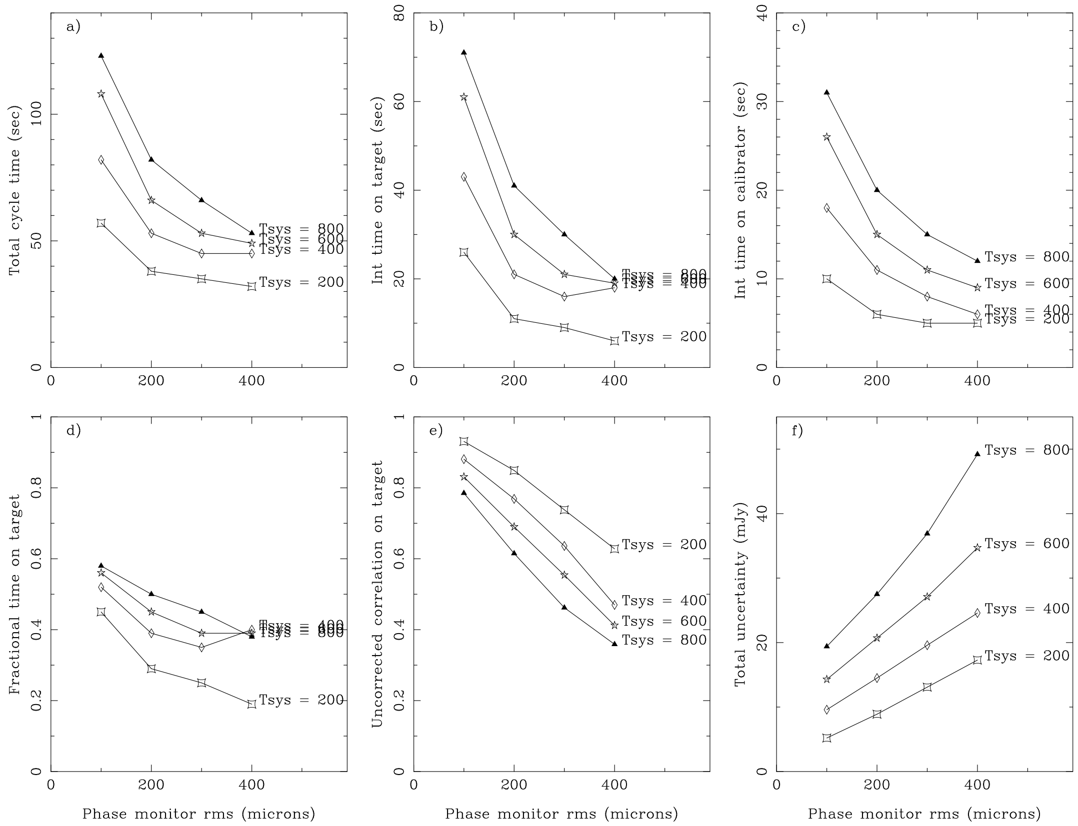

Fig. 4.— The optimal cycle time as a function of system temperature and rms path as measured by the phase monitor. The variables plotted on the y-axis are: a) total cycle time, b) total time on target, c) total time on calibrator (note different scale), d) fractional time on target within a cycle, e) the uncorrected correlation on target for the rms phase for this cycle time, and f) the total uncertainty (per bin) on the target.

parameters. As seen in Table 1, the cycle times are all roughly 40–60 seconds, although the target and calibrator integration times do vary. As the decorrelation uncertainty is multiplied by F_{target} [Eq. 4], the total uncertainty is strongly tied to the target strength. The strength of the test calibrator and the strength and distance of the phase calibrator are all important, but as these values are known ahead of time for a given target, the integration times can be adjusted accordingly. A weaker, nearby calibrator or a stronger, farther one have similar t_{cyc} and total uncertainty, however the target and calibrator integration times are very different (compare lines 7 and 10).

Of the parameters in the atmospheric model, the wind speed has the largest effect on the optimal cycle time (lines 4 and 5 of Table 2). This is because the wind speed * t_{cyc} term dominates the magnitude of the phase fluctuations (see §2). The altitude and thickness of the turbulent layer, which are not well determined, do not change the optimal cycle time significantly. I also changed how often the test calibrator was observed, from every 3 to every 5 target cycles (default

Source parameters					Results				
F_{source} (Jy)	n_{bins}	F_{test} (Jy)	F_{cal} (Jy)	d_{cal} (deg)	t_{cyc} (sec)	t_{target} (sec)	t_{cal} (sec)	Correlation on target	σ_{total} (mJy)
0.1	3	0.4	1	10	45	15	9	0.81	11.6
0.05	3	0.4	1	10	53	24	8	0.78	8.2
0.2	3	0.4	1	10	45	13	11	0.82	19.5
0.1	**1**	0.4	1	10	41	10	10	0.84	9.1
0.1	**10**	0.4	1	10	53	24	8	0.79	15.8
0.1	3	**0.2**	1	10	49	19	9	0.81	12.7
0.1	3	**0.6**	1	10	45	15	9	0.82	11.0
0.1	3	0.4	**0.5**	10	57	18	18	0.74	14.2
0.1	3	0.4	**2**	10	41	15	5	0.86	9.8
0.1	3	0.4	1	**5**	41	16	10	0.87	9.4
0.1	3	0.4	1	**20**	60	17	8	0.72	15.5

Table 1: Effect of changing different target and calibrator parameters on the optimal cycle time. A system temperature of 300 K and a rms path of 200 μm were used. The value listed for the correlation is the uncorrected value. The parameter in bold face has been altered from the standard case (line 1).

Atmosphere parameters				Results				
Altitude (km)	Thickness (km)	Wind sp (m/sec)	Baseline (km)	t_{cyc} (sec)	t_{target} (sec)	t_{cal} (sec)	Correlation on target	σ_{total} (mJy)
1	0.5	5	1	45	15	9	0.81	11.6
0.5	0.5	5	1	47	17	9	0.84	10.4
2	0.5	5	1	44	15	8	0.77	13.3
1	**0.25**	5	1	45	15	9	0.80	12.0
1	**1**	5	1	49	18	10	0.82	11.3
1	0.5	**2.5**	1	59	26	12	0.88	8.6
1	0.5	**10**	1	38	11	6	0.71	15.8

Table 2: Effect of changing the altitude and thickness of the turbulent layer and the wind speed on the optimal cycle time. The target parameters are those given on line 1 of Table 1. A system temperature of 300 K and a rms path of 200 μm were used. The parameter in bold face has been altered from the standard case (line 1).

is every 4 cycles), which did not alter the cycle time.

The system temperature and the rms path, which are not known in advance, significantly affect t_{cyc} (Figure 4). However, both can be measured during the observations and the cycle time altered appropriately. To test to importance of a flexible script, I chose a standard cycle of 15 seconds on target and 10 seconds on the calibrator and calculated the total uncertainty for a range of system temperatures and rms path values (Figure 5). The solid lines show σ_{total} for the 15/10 second cycle and the dotted lines are σ_{total} for the optimal cycle time. The uncertainty is similar for most values of T_{sys} and rms path suggesting that once the optimal t_{cyc} is known for a given set of target and calibrator parameters, that value of t_{cyc} will be adequate for most A array observing conditions. The largest increases in σ_{total} are $\sim$25% and occur at high T_{sys} with low rms path or low T_{sys} and high rms path.

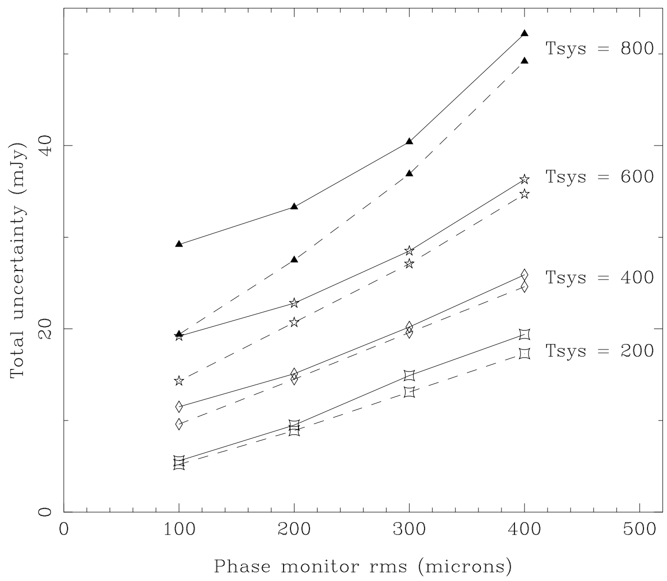

Fig. 5.— The total uncertainty as a function of system temperature and rms path for 15 seconds on target and 10 seconds on the calibrator (solid line) and for the optimal cycle (dashed line).

In these fast switching cycle times, the overhead from the slew and settle times is generally almost half of the total cycle. Decreasing the settle time to 2 seconds, possibly by raising the pointing requirement, would decrease the cycle time for the test case discussed above to 38 seconds, decreasing σ_{total} by 5%. If the slew rate is doubled to 3 degrees/second, σ_{total} decreases by 10% for a target-calibrator distance of 10°. Making both of these improvements results in a 15% decrease. Although these seem like minor improvements, recall that to produce a 15% decrease in the thermal noise alone requires 40% more integration time. If the slewing and settling times are a few seconds longer than assumed, σ_{total} increases by a similar percentage.

4.3. Observational tests of parameters

Some of the assumptions detailed in §3 can be tested observationally. In particular, the temporal and spatial variations in the decorrelation should be measured to test if the 25% accuracy in rms phase as derived from phase monitor data still holds on shorter time scales and longer baselines. Also, the two methods of observing the test calibrator (within the cycle or in a separate cycle) should be tested for accuracy in measuring the rms phase. In real observations, the target and the test calibrator will have somewhat different distances to the phase calibrator and this may effect the estimation of the rms phase. As the phase fluctuations are a function of elevation, observing a test calibrator located at a much higher or lower elevation than the target may decrease the accuracy in estimating the decorrelation. Optimal cycle times can be re-calculated when the properties of the turbulence are better known.

4.4. Interactive program

The optimal cycle times for many target/calibrator cases can be found using Table 1 and Figure 4. For observers who would like to find the optimal cycle for their exact parameters, an interactive version of the program which produced Table 1 is provided. The inputs entered by the user are: T_{sys}, phase monitor rms path, target flux, number of bins, calibrator flux, target-calibrator distance and test calibrator flux. If the user chooses, the slew rate, settle time and uncertainty in estimating the rms phase can be altered from the default values. The output produced is the optimal target and calibrator integration times and a plot of the *uncorrected* correlation and the total uncertainty as a function of target and calibrator integration time (Figure 6).

Currently the program can be run on `ral.berkeley.edu` on the `bima` account. Go to `~bima/rla` and run the script `cycle_time.csh`. The plot can be output either to the screen or saved to a postscript file. A brief explanation of the program and inputs is given in `cycle_time.README`.

5. Recommendations

The optimal cycle time for A array observations depends on many atmospheric and source properties, some of which may not be known before the observations. However, this study demonstrates that for many of the cases studied, the optimal cycle times are similar. The following recommendations are based on the assumptions detailed in §3. Estimates for cycles time at λ=1.3 mm can be made by considering the results in Figure 4 for higher system temperatures and by doubling the actual rms path to account for the increased phase fluctuations at higher frequencies ($\phi_{atm} \propto \nu$).

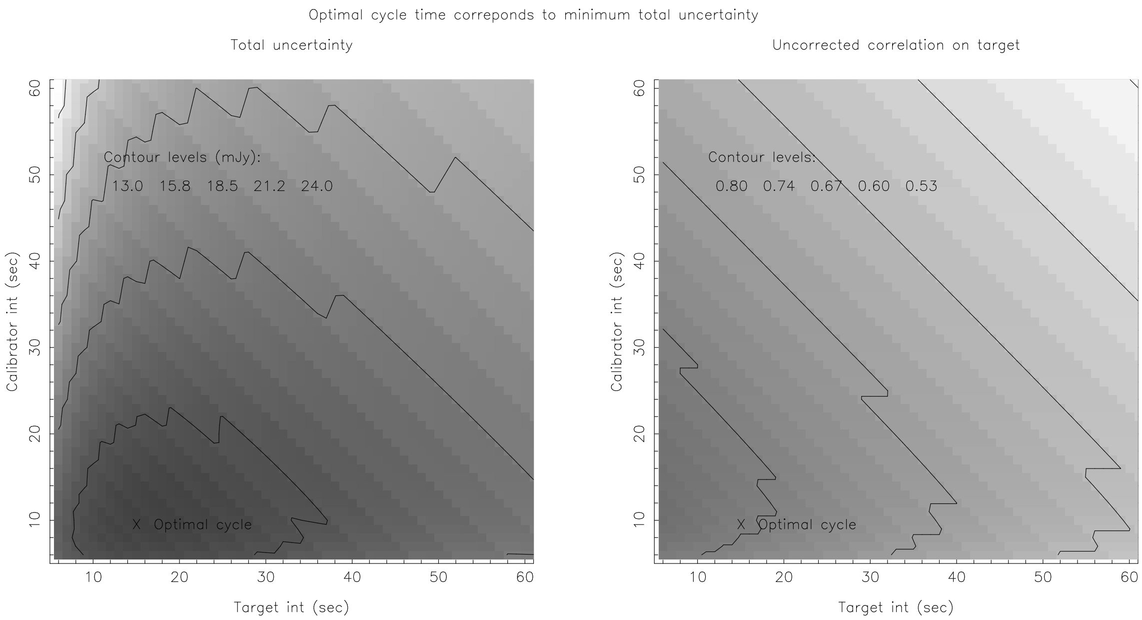

Fig. 6.— Example output plot from *cycle_time*. The uncorrected correlation on the target source and the total error are plotted as a function of the integration time on the target and on the calibrator.

1. Given the decorrelation present in all but the best weather conditions (Figure 1), a test calibrator should be used to estimate the decorrelation.

2. In 'standard' A array weather (T_{sys} = 300 K and rms path of 200 μm) the optimal cycle time at λ=3mm is roughly 45 seconds with 15 seconds on target and 10 seconds on the calibrator.

3. Once the cycle time has been calculated for a given set of target and calibrator parameters, that cycle time should be sufficient for most suitable system temperatures and rms path values.

4. For observations with higher system temperatures (low declination sources or observations near 115 GHz) the cycle time should be *increased*.

5. For observations during weather with larger rms path variations (300–400 μm), the cycle time should be *decreased*.

6. Good A array observations (without self-calibration) will be very difficult for rms path values > 400 μm.

References

Akeson, R.L., 1998, BIMA Memo #68.

Lay, O.P., 1997, A&A, 112, 535.

Lay, O.P., 1998, in preparation.

Wright, M.C.H., 1996, PASP, 108, 520.